Wildfire responses to abrupt climate change in North America

J. R. Marlon[a,1], P. J. Bartlein[a], M. K. Walsh[a], S. P. Harrison[b], K. J. Brown[c,d], M. E. Edwards[e,f], P. E. Higuera[g], M. J. Power[h], R. S. Anderson[i], C. Briles[g], A. Brunelle[h], C. Carcaillet[j], M. Daniels[k], F. S. Hu[l], M. Lavoie[m], C. Long[n], T. Minckley[o], P. J. H. Richard[p], A. C. Scott[q], D. S. Shafer[r], W. Tinner[s], C. E. Umbanhowar, Jr.[t], and C. Whitlock[g]

[a]Department of Geography, University of Oregon, Eugene, OR 97403; [b]School of Geographical Sciences, University of Bristol, Bristol BS8 1SS, United Kingdom; [c]Department of Quaternary Geology, Geological Survey, Denmark and Greenland, Øster Voldgade 10, DK-1350 Copenhagen, Denmark; [d]Royal British Columbia Museum, Victoria, BC, Canada V8W 9W2; [e]School of Geography, University of Southampton, Southampton SO17 1BJ, United Kingdom; [f]Alaska Quaternary Center, University of Alaska, Fairbanks, AK 99775; [g]Department of Earth Science, Montana State University, Bozeman, MT 59717; [h]Department of Geography, University of Utah, Salt Lake City, UT 84112; [i]Center for Sustainable Environments and [k]Ecological Restoration Institute, Northern Arizona University, Flagstaff, AZ 86011; [j]Centre for Bio-Archeology and Ecology (Unité Mixte de Recherche 5059, Centre National de la Recherche Scientifique) and Paleoenvironments and Chronoecology, Institut de Botanique, Université Montpellier 2, 163 Rue Broussonet, F-34090 Montpellier, France; [l]Departments of Plant Biology and Geology, University of Illinois at Urbana–Champaign, Urbana, IL 61801; [m]Département de Géographie et Centre d'Études Nordiques, Université Laval, Québec, QC, Canada G1V 0A6; [n]Department of Geography and Urban Planning, University of Wisconsin, Oshkosh, WI 54903; [o]Department of Botany, University of Wyoming, Laramie, WY 82071; [p]Département de Géographie, Université de Montréal, C. P. 6128 Centre-ville, Montréal, QC, Canada H3C 3J7; [q]Department of Earth Sciences, Royal Holloway, University of London, Egham, Surrey TW20 0EX, United Kingdom; [r]Division of Hydrologic Sciences, Desert Research Institute, Nevada System of Higher Education, 755 East Flamingo Road, Las Vegas, NV 89119; [s]Institute of Plant Sciences and Oeschger Centre for Climate Change Research, University of Bern, Altenbergrain 21, CH-3013 Bern, Switzerland; and [t]Biology and Environmental Studies, St. Olaf College, Northfield, MN 55057

Edited by Christopher B. Field, Carnegie Institution of Washington, Stanford, CA, and approved December 29, 2008 (received for review August 19, 2008)

It is widely accepted, based on data from the last few decades and on model simulations, that anthropogenic climate change will cause increased fire activity. However, less attention has been paid to the relationship between abrupt climate changes and heightened fire activity in the paleorecord. We use 35 charcoal and pollen records to assess how fire regimes in North America changed during the last glacial–interglacial transition (15 to 10 ka), a time of large and rapid climate changes. We also test the hypothesis that a comet impact initiated continental-scale wildfires at 12.9 ka; the data do not support this idea, nor are continent-wide fires indicated at any time during deglaciation. There are, however, clear links between large climate changes and fire activity. Biomass burning gradually increased from the glacial period to the beginning of the Younger Dryas. Although there are changes in biomass burning during the Younger Dryas, there is no systematic trend. There is a further increase in biomass burning after the Younger Dryas. Intervals of rapid climate change at 13.9, 13.2, and 11.7 ka are marked by large increases in fire activity. The timing of changes in fire is not coincident with changes in human population density or the timing of the extinction of the megafauna. Although these factors could have contributed to fire-regime changes at individual sites or at specific times, the charcoal data indicate an important role for climate, and particularly rapid climate change, in determining broad-scale levels of fire activity.

biomass burning | charcoal | comet | Younger Dryas

It is generally asserted that anthropogenic climate change will lead to widespread and more frequent fires (1, 2). Data from western North America in recent decades are consistent with this; they show that increases in the frequency of wildfire and the duration of the fire season are linked to increased spring and summer temperatures and earlier spring snowmelt (3). Changes in the pattern of precipitation are likewise affecting fire activity (4), as is the development of high fuel loads associated with long-term fire suppression (5). The effects of climate variability on fuels and fire regimes on multiple time scales have received much attention (6–8), and some research has linked shifts in fire regimes at individual sites to rapid climate changes (9). However, the broad-scale response of wildfires to large, abrupt climate changes in the past has received little attention (10, 11). One period of particular interest is the last glacial–interglacial transition (LGIT, 15–10 ka), when large and sometimes abrupt (i.e., decades to centuries) changes in climate and biota occurred in many parts of North America. In some regions, environmental changes at the beginning and end of the Younger Dryas chronozone (YDC) (12.9–11.7 ka) (12), in particular, were larger than those at any subsequent time (13). Such changes are similar in terms of the magnitude and rate of change to those projected for the future (14–16) and thus provide an opportunity to examine the response of fire regimes to rapidly changing environmental conditions in a variety of settings.

Investigating wildfire activity during the LGIT also allows us to test the recent proposal that a catastrophic extraterrestrial impact event at ≈12.9 ka had "continent-wide effects, especially biomass burning" (17). Firestone *et al.* (17) proposed that a comet exploded over the Laurentide ice sheet, producing a shock wave that would have traveled across North America at hundreds of kilometers per hour, and if multiple large airbursts occurred, could have ignited many thousands of square kilometers. Firestone *et al.* (17) also hypothesized that the event triggered global cooling, and that extreme wildfires destroyed forests and grasslands and produced charcoal, soot, toxic fumes and ash. These impacts, in turn, ostensibly limited the food supplies of herbivores, contributing to the extinction of North American megafauna and forcing major adaptations of PaleoAmericans (17), although this latter point has been disputed (18).

Even without invoking catastrophic events such as a comet impact, there are still reasons to expect a broad-scale response of fire activity in North America to the abrupt climate changes during the LGIT (19–21). At the beginning of the YDC (12.9 ka), North Atlantic meridional overturning slowed or shut down (21, 22). This led to abrupt cooling in the circum-North Atlantic region and general changes in atmospheric circulation around North America (23–25). Because atmospheric circulation affects temperature, precipitation and the position of storm tracks (26,

Author contributions: J.R.M. and P.J.B. designed research; J.R.M., P.J.B., M.K.W., S.P.H., K.J.B., M.E.E., P.E.H., M.J.P., R.S.A., C.B., A.B., C.C., M.D., F.S.H., M.L., C.L., T.M., P.J.H.R., D.S.S., W.T., C.E.U., and C.W. performed research; J.R.M., P.J.B., M.K.W., S.P.H., K.J.B., M.E.E., P.E.H., and M.J.P. analyzed data; and J.R.M., P.J.B., M.K.W., S.P.H., K.J.B., M.E.E., P.E.H., M.J.P., R.S.A., C.B., A.B., C.C., M.D., F.S.H., M.L., C.L., T.M., P.J.H.R., A.C.S., D.S.S., W.T., C.E.U., and C.W. wrote the paper.

The authors declare no conflict of interest.

This article is a PNAS Direct Submission.

[1]To whom correspondence should be addressed. E-mail: jmarlon@uoregon.edu.

This article contains supporting information online at www.pnas.org/cgi/content/full/0808212106/DCSupplemental.

27), the particularly abrupt onset of the YDC was registered across the continent. A large, rapid climate reversal occurred in regions adjacent to the North Atlantic, whereas more distant regions registered changes in the progress of the LGIT (19, 28, 29). Other abrupt climate transitions focused on the North Atlantic, such as the onset of the Bølling–Allerød interval (14.7 ka), or short climatic oscillations, such as the intra-Allerød cold period (IACP) (≈13.2 ka), may also have had continent-wide impacts on climate.

Large-amplitude, rapid climate change affects fire regimes directly by altering the patterns of ignition and fire weather (30) and indirectly through vegetation composition (19, 31, 32), a major determinant of landscape flammability (33). The nature of the changes in ignition, fire weather, and vegetation composition will not be homogenous at a regional scale, but any rapid climate change, whatever its direction, imposes stress on an ecosystem and can trigger some change in the fire regime. Stress would result in increased mortality of the woody vegetation and a buildup of fuel, for example, as a result of pest outbreaks or physiological intolerance of new climate extremes (50). The rate at which such factors affect the fire regime varies, so a broad-scale change in fire activity would not necessarily exhibit absolute synchroneity, but some change should still be evident at most sites.

Charcoal and pollen from 35 lake-sediment records across North America [see supporting information (SI) Fig. S1 and Table S1] were used to assess changes in fire activity (defined here as biomass burned and fire frequency) and woody biomass during the LGIT. Variations in charcoal abundance or influx (particles/cm^2/yr) provide a record of past trends in biomass burning (34–37). Fifteen high-resolution macroscopic charcoal records (i.e., <50 years per sample and particles >100 μm) were further analyzed to reconstruct past fire episodes (defined as 1 or more fires occurring during the time spanned by a charcoal peak) (36, 38) and charcoal peak magnitude, an assumed metric of fire size, severity, or proximity (39) (*SI Methods*). The proportion of arboreal pollen (AP) in the lake sediments, which reflects the abundance of tree and shrub taxa on the landscape, was used to estimate the levels of woody biomass in the vegetation at the sites. AP can overestimate tree cover and mask shifts in trees and shrubs (40), so we consider it only a general indicator of available woody fuels. Records of charcoal influx, peak frequency, and AP were used to document trends in biomass burning (35, 36), fire-episode frequency (hereafter termed fire frequency), and woody fuel levels. These trends were compared with ice-core records of CO_2 (41) and $\delta^{18}O$ (21), the latter clearly illustrating abrupt climate changes, to explain the broad-scale changes in fire activity.

Results and Discussion

Trends in Fire Regimes and Woody Fuels. The general trend of charcoal influx across all sites (as represented by a 3-segment linear regression, Fig. 1*C*) indicates a significant ($P < 0.01$) increase in biomass burning until the beginning of the YDC, no overall change during the YDC, and then a further increase in biomass burning thereafter ($P < 0.01$). A local regression curve, which does not assume a specific form for the trend, displays a similar pattern. The bootstrap confidence intervals around charcoal influx indicate that these trends are not induced by any particular record. Inspection of the records (Fig. 2 and Fig. S2), however, shows that there can be different responses at individual sites reflecting modulation of the regional-scale response by local factors. For example, whereas sites 4–9 in southern British Columbia (BC) all show increasing biomass burning from 15 to 10 ka, spatial patterns are complex in the Pacific Northwest, Sierra Nevada, and Northern U.S. Rocky Mountains (NRM). The 3 sites in Alaska (AK) show increasing burning during the Bølling–Allerød and stable levels during the YDC, but trends are variable after the YDC. Almost no spatial coherence is evident in the Southwest, Midwest, and East, although these regions have limited data. Thus, whereas the composite record strongly indicates broad-scale trends in biomass burning, heterogeneity is expected and apparent at local to regional scales.

The overall trend in fire frequency increases during the Bølling–Allerød (Fig. 1*D*, Fig. S3) and has no discernable trend thereafter. Some regions show coherent patterns in fire frequency, including AK (sites 1 and 2), the Pacific Northwest (sites 11, 13, and 14), and the NRM (sites 21–23, and 25) (Fig. S3), although the nature of the changes naturally differ between regions. Fire frequency is most variable after 11.7 ka; only sites 21 and 29 show little or no change after that time. In general, peaks in fire frequency tend to match local maxima in biomass burning (e.g., at 13.9, 13.1, 12.3, and 11.7 ka).

There are no empirical studies that link the absolute size of charcoal peaks to a specific fire characteristic, such as area burned or severity, so the peak magnitudes must be interpreted with caution (Fig. S3). However, in previous research, unusually large peaks have been linked to extreme fire years in the historical record when large areas burned at the regional scale (42, 43). For example, fires in 1910 that burned >400,000 ha in the NRM comprised the largest peak of the last 120 years at site 20 (42). Consequently, peak-magnitude data suggest that many large fire episodes occurred between 15 and 10 ka, and large or severe fire episodes were more likely after the end of the YDC than before it, as for example in the Pacific Northwest (sites 11–13), the NRM (sites 20, 23–25), and the Southwest (site 27) (Fig. S3). Fire frequency was also high at most of these sites after the YDC.

The woody biomass trend increases during the Bølling–Allerød, is stable during the YDC, and decreases thereafter (Fig. 1*E*). Trends at individual sites again vary regionally and with elevation (Fig. 2 and Fig. S2). Woody biomass declines at most sites in BC and increases in the Sierra Nevada, Southwest, and Northeast. Other regions show mixed patterns. Fire–fuel relationships among sites also show regional similarities. For example, trends in charcoal influx and AP are similar at mid- to high-elevation sites in the Pacific Northwest and NRM (sites 13, 15, 23, 24, and 25), where biomass burning and woody fuel levels generally increased together as open forests became more closed or alpine vegetation was replaced by parkland and then forest during the LGIT (8). In BC (i.e., at sites 5, 6, 7, 8, and 10), an inverse relationship in fire and fuels is apparent because biomass burning increased as closed mixed conifer forests were replaced by more open forests (44). Charcoal influx is often opposite to AP in the Midwest as well, where grass abundance (low woody biomass) is a good predictor of biomass burning (45). Important changes in woody fuel levels in AK are obscured in the AP trends, because AP does not show changes in the relative importance of shrubs versus trees. AP declines at site 3 at 11 ka, for example, despite a large increase in *Populus* at that time (63). Overall, the spatiotemporal variability in woody fuel levels and biomass burning makes it difficult to generalize about fire–climate–vegetation linkages at the continental scale, but the role of climate in determining both woody fuel levels and fire activity underpins the regional coherence in charcoal–AP relationships. The AP data do indicate that availability of woody fuels was not a limiting factor in determining levels of biomass burning at the beginning or end of the YDC.

Evidence for Continent-Wide Wildfires at 12.9 ka. Firestone *et al.* (17) hypothesized that a comet impact at 12.9 ka ± 50 y triggered continental-scale wildfires across NA. One specific example has been proposed by Kennett *et al.* (46). However, the well-documented rapid climate changes of this time alone may have triggered increased fire at a regional scale. To separate these effects, we compared the response of fire during intervals of rapid climate changes at the beginning and at the end of the YDC. Fire-episode events that occurred during the transitions

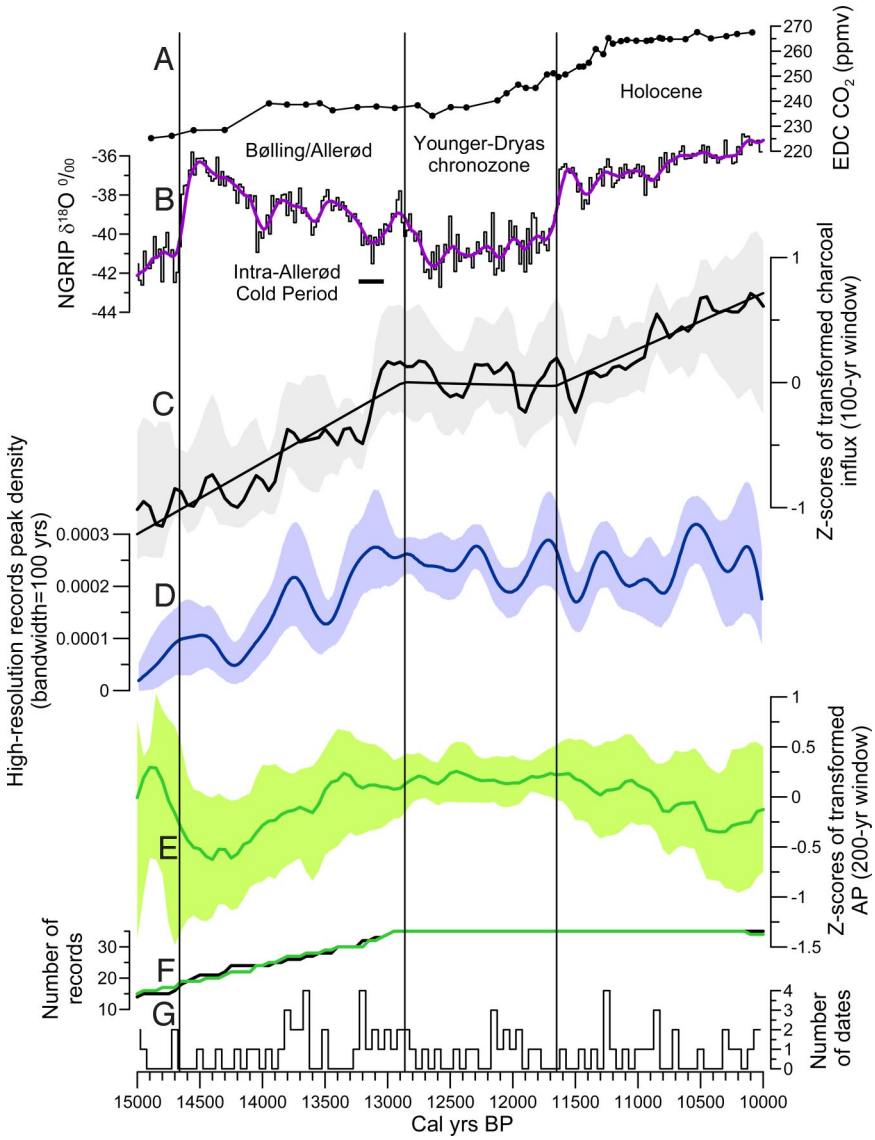

Fig. 1. Reconstructions of biomass burned, fire frequency, and woody biomass levels in North America. (*A*) The CO_2 ice-core record from Antarctica (41). (*B*) The NGRIP $\delta^{18}O_{ice}$ record, a proxy for North Atlantic temperatures (21). (*C*) Reconstruction of biomass burned based on 35 records; the straight lines are segmented regression curves, and the smooth curves are local-regression fitted values. (*D*) Reconstruction of fire frequency based on 15 high-resolution records, expressed as the density of peaks per site-year. (*E*) Trends in woody biomass based on 35 records. (*F*) Number of records contributing to the biomass burning (black) and woody biomass (green) trends. (*G*) Number of dates per 50-year interval in the 35 paleo records. Confidence intervals (95%) are based on bootstrap resampling of sites. Vertical lines mark the beginning (≈12.9 ka) and ending (≈11.7 ka) of the YDC.

into and out of the YDC were identified in both the high- and low-resolution records (see *Methods*) to determine whether fire episodes, regardless of magnitude, were more likely to occur (within ±50 y) at 12.9 ka than at 11.7 ka (Figs. 1*A* and 2). Because of high uncertainties in radiocarbon dating during the YDC, both 100- and 500-y window widths were used to identify fire episodes (Fig. 2). By using a 100-y window, 13 sites across the continent (Fig. 2) showed a peak (or increasing charcoal if no sample was within the window) at 12.9 ka. The peak was large (i.e., >90th percentile based on quantile regression) in the 9 low-resolution records, but it was not present in any of the 5 high-resolution records that registered a peak at 12.9 ka (±50 y) (Fig. S3), suggesting that the relatively high magnitude of fires at 12.9 in the low-resolution sites may be an artifact of the small number of samples in these records. The data also indicate that only 3 sites showed a peak only at 12.9 ka, whereas 12 sites showed a peak only at 11.7 ka, the abrupt end of the YDC (Fig. 2 and Figs. S1 and S3). Using a large 500-y window width greatly increased the number of sites recording fires ≈12.9 ka; however it also increased the number of fire episodes recorded at 11.7 ka (Fig. 2). It could be argued that poor dating control on some of the records prevented identification of fire episodes at 12.9 ka; however, when we limited our analysis to the 14 records with dates within ±300 years of 12.9 ka (Fig. 2), the results did not change. Peaks in charcoal influx were registered throughout the LGIT, particularly associated with abrupt climate changes, but there was no evidence of continent-wide wildfires at the beginning of the YDC.

Potential Controls on Fire Regimes and Woody Fuel Levels During the LGIT. The broad-scale trends in biomass burning, fire frequency and magnitude, and woody fuels during deglaciation are consistent with climate changes documented by ice cores, marine and lake sediments, speleothem, and other records from North America (21, 28, 47, 48). During the Bølling–Allerød, woody

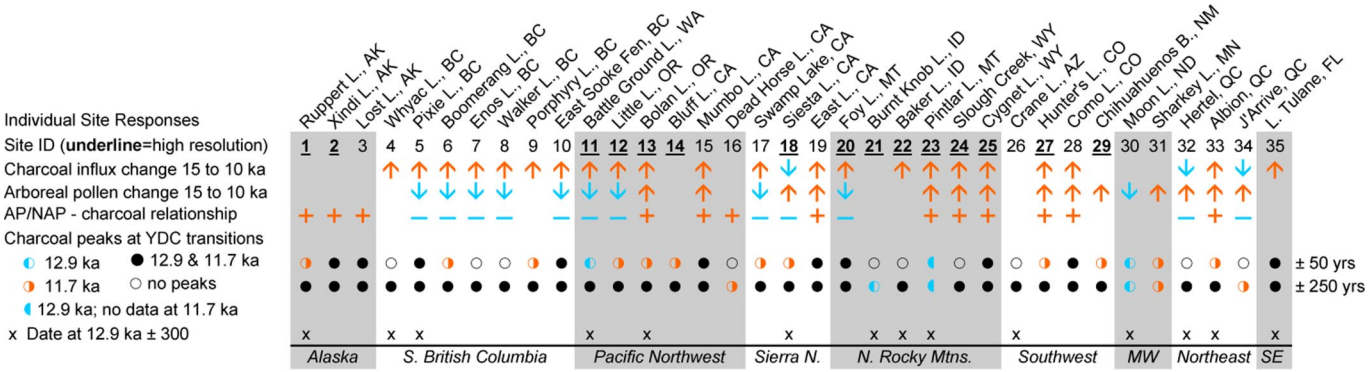

Fig. 2. Site summaries of changes in charcoal influx, arboreal pollen (AP), and charcoal–pollen relationships during the LGIT and of charcoal peaks at the beginning and end of the YDC. High-resolution site numbers are in bold type and underlined. Regions are identified by alternate shading. A ↑ (↓) indicates a general upward (downward) trend in charcoal influx. A + (−) indicates a positive (negative) relationship between charcoal and AP. Records that had a radiocarbon or tephra date within 300 years of 12.9 ka are marked by an x in the bottom row.

biomass, biomass burning, and fire frequency all increased (Fig. 1*E*), a likely consequence of warming and increased tree cover (40). A stepped increase in biomass burning is evident at 13.9 ka, coincident with a short period of warming and is matched by a peak in fire frequency.

A particularly steep increase in charcoal influx occurred at 13.2 ka (Fig. 1*C*); this is the largest and most rapid change in biomass burning during deglaciation. Burning was widespread but not continent wide (see site details in *SI Methods*). Furthermore, the change in fire regime is not unique: Several sites show similar peaks before the onset of the YDC, and many show an even larger peak at the end of the YDC. The widespread increase in fire activity (i.e., charcoal influx and peak frequency) at 13.2 ka appears ≈300 years before the hypothesized comet impact (17). Of the sites that do show fire activity at 13.2 ka, many are from regions distant from the proposed locus of the impact area over the Laurentide ice sheet, as well as from the proximal influence of the ice sheet on regional climates (e.g., in AK, the Southwest, Pacific Northwest, and the NRM). The timing and distribution of fire activity at 13.2 ka is consistent with the IACP—an abrupt short-term climate reversal recorded in the GISP $\delta^{18}O$ ice-core data (Fig. 1*B*). The IACP is associated with a rapid oscillation in North Atlantic temperatures that may have affected atmospheric circulation patterns across the continent (21, 23, 49) and increased the likelihood of drought as well as severe frost damage on some tree species (50). Any increase in vegetation mortality associated with such events would have added to the available fuels and facilitated an increase in fire.

During the YDC, ice-core $\delta^{18}O$ data indicate cool and variable temperatures in the North Atlantic region. Cooling is also evident in parts of western North America based on pollen and speleothem records (25, 28, 49), but climate patterns likely varied across the continent (27). The composite records (Fig. 1) show that biomass burning was higher but more variable than before 13.2 ka. Fire frequency and biomass burning had local maxima at ≈12.3 ka and at the end of the YDC (11.7 ka). Although there are fundamental and widespread changes in vegetation at the beginning (and end) of the YDC (19), the woody biomass trend shows little change during the YDC. This lack of change does not preclude change in specific regions e.g., Alaska (48) or at individual sites.

Biomass burning and fire frequency both decline at 11.7 ka but increase thereafter. Woody biomass, however, decreases from 11.7 to 10.0 ka. This contrast in behavior marks a shift in the relationship between fire and vegetation. Before 11.7 ka, woody biomass and fire activity generally change in parallel; after 11.7 ka, they change in opposite directions. Early-Holocene warming and enhanced seasonality facilitated the emergence of new vegetation communities and disturbance patterns (19, 32, 51). Low-elevation sites in the western US show the biggest changes, with declining woody biomass as forests became more open (44, 52) and more likely to burn (Fig. S2 and Fig. 2). High-elevation sites in the Pacific Northwest and NRM also show increasing fire activity but in association with increasing rather than decreasing woody fuel levels. New fire–fuel patterns also evolved in the Northeast after the YDC, with declines in biomass burning associated with increases in woody biomass.

Factors other than climate may have contributed to observed changes in fire regimes during the LGIT, including changes in atmospheric CO_2, the arrival of Clovis people between ≈13.4 and 12.8 ka (53), and the extinction of herbivorous megafauna (54). Changes in CO_2 affect vegetation productivity (55) and potentially fuel loads. Atmospheric CO_2 increased in stepwise fashion from the Last Glacial Maximum to the beginning of the Holocene (56) (Fig. 1*A*). The changes in woody biomass, fire frequency, and biomass burning are not coincident with changes in CO_2, although increasing CO_2 may have contributed to woody biomass production during the early part of the Bølling–Allerød. Clovis people appeared in North America between 13.4 and 12.8 ka, broadly coincident with the sharp increase in biomass burning at 13.2 ka, and then rapidly spread out across the continent (18). Paleoindians may have increased fire activity directly by setting more fires (57) or indirectly by reducing megafaunal populations. The decline in megafaunal populations, in turn, could have increased fuel loads and changed soil moisture regimes, both of which could have promoted fire (58, 59). There is some evidence for an association between megafaunal declines based on *Sporormiella* data and increased burning in the Northeast (58).

The 13.2 ka fire peak is registered at sites widely dispersed across the continent; it is not consistent with the progressive colonization of North America by Paleoindians. It also seems unlikely that people (or megafauna) would have caused an increase in burning across the full range of elevations represented by the sites and particularly at high-elevation sites (the fire peak is evident at 5 sites >2,000 m; see *SI Methods* and Table S1). Furthermore, most fire records show discrete peaks rather than permanent regime changes, as might be expected if humans or megafauna exerted a major control on fire regimes. It is possible, however, that the arrival of people and/or the extirpation of megafauna (18, 53, 54) played a role in permanently altering fire regimes at the sites that show a fundamental fire-regime shift prior to or at 13.2 ka. After 13.2 ka, fire-regime changes are not coincident with periods of increase in human populations. Thus, the spatial and temporal distribution of the

fire signal point toward climate as the primary cause of increased fire activity at 13.2 ka.

In summary, fire records from North America show stepped increases in biomass burning during the LGIT. Abrupt climate changes are generally marked by a shift in the level of burning as well as an increase in the incidence of fires. No continent-wide fire response is observed at the beginning of the Younger Dryas chronozone, the time of the hypothesized comet impact. The results provide no evidence of synchronous continent-wide biomass burning at any time during the LGIT. The data indicate variability in the direction of changes in fire regimes among paleofire records, which may be due in part to noise and local variability (60), human activity, or megafaunal declines. The distribution of charcoal peaks across time and space, however, suggests that such patterns are more likely a result of spatially complex climate controls and/or vegetation changes. Although there is broad congruence between changes in climate, fire, and human populations at the beginning of the YDC, we find no convincing evidence that the observed changes in fire activity were caused solely by changes in human or herbivorous megafauna populations.

Methods

We used 30 lake-sediment records in North America from the Global Charcoal Database (GCD v. 1*[†]) and 5 records from authors that (*i*) were recording fire activity before, during, and after the YDC; (*ii*) had at least 5 data points and one date (radiocarbon or tephra) from 10 to 15 ka; and (*iii*) had pollen data from the same site. We did not include charcoal data from records that only sampled the beginning of the YDC because there is no baseline for analyzing changes in the fire regime with such data (46). We also excluded marine charcoal data (61) because there is no evidence that charcoal influx and peaks in influx in such records reflect recent fire activity from a consistent source region. Pollen data were obtained from authors or from the North American Pollen Database[‡] (Table S1). We examined the chronologies for each record to ensure that the age–depth relationships were generally consistent throughout the LGIT and that no age reversals occurred during that interval. Under such conditions, age controls in lake-sediment records are sufficient to describe centennial-scale variations (see *SI Methods*).

For all analyses, charcoal concentration data (particles cm^{-3}) were converted to influx values (particles cm^{-2} y^{-1}) (see *SI Methods*). For the low-resolution records, millennial-scale (background) trends were identified by smoothing the data by using quantile regression (62). Any increase in charcoal influx above background within a defined interval (i.e., either ±50 or ±250 years) was considered a peak. High-resolution records were smoothed by using a decomposition technique (63) that separates peaks from background charcoal and allows the reconstruction of peak magnitude and fire frequency. Arboreal pollen proportions were obtained by dividing the sum of arboreal and shrub pollen percentages (AP) by the sum of the total terrestrial pollen percentages [AP/(AP + NAP)].

To display the general trends in the charcoal influx, the data were transformed to stabilize the variance and standardized to facilitate comparisons across a range of charcoal influx levels (37). To assess the significance in the trend, we fit a segmented linear regression model to these data, with breakpoints at the beginning and end of the YDC (see *SI Methods*). We also summarized the data by using ''lowess'' or local regression curves. Confidence intervals for the local regression curves were generated by a bootstrap approach in which individual records (not samples) were sampled with replacement over 1,000 replications. The approach reveals the sensitivity of the trends to the particular selection of charcoal and pollen records used here. Pollen data were also transformed (64) and summarized by using local regression curves. The peak frequency trends in the high-resolution records were summarized by a local-density (kernel smoothing) procedure.

ACKNOWLEDGMENTS. We thank Jack Williams for providing pollen data, Jake Bartruff for map assistance, D. Burney, D. Gavin, D. J. Meltzer, and D. K. Grayson for discussions, and 2 anonymous reviewers for comments that greatly improved the manuscript. This work was supported by U.S. National Science Foundation Paleoclimatology and Geography and Regional Science Program Grants ATM-0117160, ATM-0714146, and BCS-0727424. The charcoal data are included in Global Charcoal Database Version 2 compiled by the Global Palaeofire Working Group (GPWG) of the International Geosphere–Biosphere Cross-Project Initiative on Fire. The GPWG is supported by the U.K. Natural Environment Research Council's QUEST (Quantifying Uncertainty in the Earth System) Program. Data compilation and analysis was supported by the QUEST-Deglaciation Project (M.P. and S.P.H.).

*www.ncdc.noaa.gov/paleo/impd/gcd.html.

[†]www.bridge.bris.ac.uk/projects/QUEST_IGBP_Global_Palaeofire_WG/.

[‡]www.ncdc.noaa.gov/paleo/napd.html.

1. International Panel on Climate Change (2007) in *Climate Change 2007: Impacts, Adaptation and Vulnerability. Contribution of Working Group II to the Fourth Assessment Report of the IPCC*, eds Parry ML, Canziani OF, Palutikof JP, van der Linden PJ, Hanson CE (Cambridge Univ Press, Cambridge, UK).
2. U.S. Climate Change Science Program (2008) in *Synthesis and Assessment Product 4.3*, ed Walsh MK (USCCP, Washington, DC).
3. Westerling AL, Hidalgo HG, Cayan DR, Swetnam TW (2006) Warming and earlier spring increase western US forest wildfire activity. *Science* 313:940–943.
4. Flannigan MD, Stocks BJ, Wotton BM (2000) Climate change and forest fires. *Sci Tot Environ* 262:221–229.
5. Schoennagel T, Veblen TT, Romme WH (2004) The interaction of fire, fuels, and climate across Rocky Mountain forests. *BioScience* 54:661–676.
6. Van der Werf GR, Randerson JT, Giglio L, Collatz GJ, Kasibhatla PS (2006) Interannual variability in global biomass burning emission from 1997 to 2004. *Atmos Chem Phys* 6:3423–3441.
7. Swetnam TW (1993) Fire history and climate change in giant sequoia groves. *Science* 262:885–889.
8. Whitlock C, *et al.* (2008) Long-term relations among fire, fuel, and climate in the north-western US based on lake-sediment studies. *Intl J Wildland Fire* 17:72–83.
9. Clark JS, Royall PD, Chumbley C (1996) The role of fire during climate change in an eastern deciduous forest at Devil's Bathtub, New York. *Ecology* 77:2148–2166.
10. Bird MI, Cali JA (1998) A million-year record of fire in sub-Saharan Africa. *Nature* 394:767–769.
11. Daniau A-L, *et al.* (2007) Dansgaard–Oeschger climatic variability revealed by fire emissions in southwestern Iberia. *Quat Sci Rev* 26:1369–1383.
12. Steffensen JP, *et al.* (2008) Abrupt climate change happens in few years high-resolution Greenland ice core data show. *Science* 321:680–684.
13. Shuman B, Bartlein PJ, Webb T (2005) The magnitudes of millennial- and orbital-scale climatic change in eastern North America during the Late Quaternary. *Quat Sci Rev* 24:2194–2206.
14. Flannigan MD, Logan KA, Amiro BD, Skinner WR, Stocks BJ (2005) Future area burned in Canada. *Clim Change* 72:1–16.
15. Williams JW, Jackson ST, Kutzbach JE (2007) Projected distributions of novel and disappearing climates by 2100 A.D. *Proc Natl Acad Sci USA* 104:5738–5742.
16. Girardin MP, Mudelsee M (2008) Past and future changes in Canadian boreal wildfire activity. *Ecol Appl* 18:391–406.
17. Firestone RB, *et al.* (2007) Evidence for an extraterrestrial impact 12,900 years ago that contributed to the megafaunal extinctions and the Younger Dryas cooling. *Proc Natl Acad Sci USA* 104:16016–16021.
18. Buchanan B, Collard M, Edinborough K (2007) Paleoindian demography and the extraterrestrial impact hypothesis. *Proc Natl Acad Sci USA* 105.
19. Shuman B, Webb III T, Bartlein PJ, Williams JW (2002) The anatomy of a climatic oscillation: Vegetation change in eastern North America during the Younger Dryas chronozone. *Quat Sci Rev* 21:1763–1916.
20. Mayewski PA, *et al.* (1993) The atmosphere during the Younger Dryas. *Science* 261:195–197.
21. Alley RB (2000) The Younger Dryas cold interval as viewed from central Greenland. *Quat Sci Rev* 19:213–226.
22. Carlson AE, *et al.* (2007) Geochemical proxies of North American freshwater routing during the Younger Dryas cold event. *Proc Natl Acad Sci USA* 104:6556–6561.
23. Taylor KC, *et al.* (1993) The ''flickering switch'' of late Pleistocene climate change. *Nature* 361:432–436.
24. Hughen KA, Overpeck JT, Peterson LC, Turmbore S (1996) Rapid climate changes in the tropical Atlantic region during the last deglaciation. *Nature* 380:51–54.
25. Reasoner MA, Jodry MA (2000) Rapid response of alpine timberline vegetation to the Younger Dryas climate oscillation in the Colorado Rocky Mountains. *Geology* 28:51–54.
26. Rutter NW, Weaver AJ, Rokosh D, Fanning AF, Wright DG (2000) Data-model comparison of the Younger Dryas event. *Can J Earth Sci* 37:811–830.
27. Yu Z, Wright HE, Jr (2001) Response of interior North America to abrupt climate oscillations in the North Atlantic region during the last deglaciation. *Earth Sci Rev* 52:333–369.
28. Vacco DA, Clark PU, Mix AC, Cheng H, Edward RL (2005) A speleothem record of Younger Dryas cooling, Klamath Mountains, Oregon, USA. *Quat Res* 64:249–256.
29. Kienast SS, McKay JL (2001) Sea surface temperatures in the subarctic Northeast Pacific reflect millennial-scale climate oscillations during the last 16 kyrs. *Geophys Res Lett* 28:1563–1566.
30. Gedalof Z, Peterson DL, Mantua NJ (2005) Atmospheric, climatic, and ecological controls on extreme wildfire years in the northwestern United States. *Ecol Appl* 15:154–174.
31. Hu FS, *et al.* (2002) Response of tundra ecosystem in southwestern Alaska to Younger-Dryas climatic oscillation. *Glob Change Biol* 8:1156–1163.

32. Anderson RR, Allen CD, Toney JL, Jass RB, Bair AN (2008) Holocene vegetation and fire regimes in subalpine and mixed conifer forests, southern Rocky Mountains, USA. *Intl J Wildland Fire* 17:96–114.
33. Agee JK (1993) *Fire Ecology of Pacific Northwest Forests* (Island Press, Washington, DC).
34. Carcaillet C, *et al.* (2002) Holocene biomass burning and global dynamics of the carbon cycle. *Chemosphere* 49:845–863.
35. Marlon J, Bartlein PJ, Whitlock C (2006) Fire-fuel-climate linkages in the northwestern USA during the Holocene. *Holocene* 16:1059–1071.
36. Higuera PE, Peters ME, Brubaker LB, Gavin DG (2007) Understanding the origin and analysis of sediment-charcoal records with a simulation model. *Quat Sci Rev* 26:1790–1809.
37. Power MJ, *et al.* (2007) Changes in fire regimes since the Last Glacial Maximum: An assessment based on a global synthesis and analysis of charcoal data. *Clim Dynam* 30:887–907.
38. Whitlock C, Bartlein PJ (2004) in *Developments in Quaternary Science* (Elsevier, Amsterdam).
39. Whitlock C, *et al.* (2006) Postglacial vegetation, climate, and fire history along the east side of the Andes (lat 41–42.5 degrees S), Argentina. *Quat Res* 66:187–201.
40. Williams JW (2002) Variations in tree cover in North America since the Last Glacial Maximum. *Glob Planet Change* 35:1–23.
41. Monnin E, *et al.* (2001) Atmospheric CO_2 concentrations over the Last Glacial Termination. *Science* 291:112.
42. Power MJ, Whitlock C, Bartlein PJ, Stevens LR (2006) Fire and vegetation history during the last 3800 years in northwestern Montana. *Geomorphology* 75:420–436.
43. Tinner W, *et al.* (1998) Pollen and charcoal in lake sediments compared with historically documented forest fires in southern Switzerland since AD 1920. *Holocene* 8:31–42.
44. Brown KJ, Hebda RJ (2002) Origin, development, and dynamics of coastal temperate conifer rainforests of southern Vancouver Island, Canada. *Can J Forest Res* 32:353–372.
45. Camill P, *et al.* (2003) Late-glacial and Holocene climatic effects on fire and vegetation dynamics at the prairie–forest ecotone in south-central Minnesota. *J Ecol* 91:822–836.
46. Kennett DJ, *et al.* (2008) Wildfire and abrupt ecosystem disruption on California's Northern Channel Islands at the Ållerød–Younger Dryas boundary (13.0–12.9 ka). *Quat Sci Rev* 27:2528–2543.
47. Barron JA, Heusser L, Herbert T, Lyle M (2003) High-resolution climatic evolution of coastal northern California during the past 16,000 years. *Paleoceanography* 18:20–21-20–19.
48. Kokorowski HD, Anderson PM, Mock CJ, Lozhkin AV (2008) A re-evaluation and spatial analysis of evidence for a Younger Dryas climatic reversal in Beringia. *Quat Sci Rev* 27:1710–1722.
49. Hu FS, *et al.* (2006) Abrupt climatic events during the last glacial-interglacial transition in Alaska. *Geophys Res Lett.* 33: L18708.
50. Tinner W, *et al.* (2008) A 700-yr record of boreal ecosystem responses to climatic variation from Alaska. *Ecology* 89:729–743.
51. Williams JW, Shuman BN, Webb T, Bartlein PJ, Leduc PL (2004) Late-quaternary vegetation dynamics in North America: Scaling from taxa to biomes. *Ecol Monogr* 74:309–334.
52. Walsh MK, Whitlock C, Bartlein PJ (2008) A 14,300-year-long record of fire–vegetation–climate linkages at Battle Ground Lake, southwestern Washington. *Quat Res* 70:251–264.
53. Meltzer DJ (2004) in *The Quaternary Period in the United States*, eds Gillespie AR, Porter SC, Atwater BF (Elsevier, Amsterdam), pp 539–563.
54. Grayson DK (2007) Deciphering North American Pleistocene extinctions. *J Anthropol Res* 63:185–214.
55. Ward JK, Tissue DT, Thomas RB, Strain BR (1999) Comparative responses of model C3 and C4 plants to drought in low and elevated CO_2. *Glob Change Biol* 5:857–867.
56. Monnin E, *et al.* (2004) Evidence for substantial accumulation rate variability in Antarctica during the Holocene, through synchronization of CO_2 in the Taylor Dome, Dome C and DML ice cores. *Earth Planet Sci Lett* 224:45–54.
57. Turney CSM, *et al.* (2001) Redating the onset of burning in Lynch's Crater (North Queensland): Implications for human settlement in Australia. *J Quat Sci* 16 Part 8:767–772.
58. Robinson GS, Burney LP, Burney DA (2005) Landscape paleoecology and megafaunal extinction in southeastern New York State. *Ecol Monogr* 75:295–315.
59. Miller GH, *et al.* (1999) Pleistocene extinction of *Genyornis newtoni*: Human impact on Australian megafauna. *Science* 283:205–208.
60. Gavin DG, Hu FS, Lertzman K, Corbett P (2006) Weak climatic control of stand-scale fire history during the late Holocene. *Ecology* 87:1722–1732.
61. Heusser L (1995) in *Proceedings of the Ocean Drilling Program, Scientific Results*, eds Kennett JP, Baldauf JG, Lyle M (Ocean Drilling Program, College Station, TX), pp 265–279.
62. Koenker R (2005) *Quantile Regression* (Cambridge Univ Press, Cambridge, UK).
63. Higuera PE, *et al.* (2008) Frequent fires in ancient shrub tundra: Implications of paleo-records for Arctic environmental change. *PLoS ONE* 3:e0001744.
64. Bartlein P, Prentice CI, Webb III T (1986) Climatic response surfaces from pollen data for some eastern North American taxa. *J Biogeog* 13:35–57.

Supporting Information

Marlon *et al.* 10.1073/pnas.0808212106

SI Methods

This file contains additional methodological details, 1 table that describes the sites in the main text, and 3 figures. Fig. S1 is a site map. Fig. S2 shows the individual records of charcoal influx and proportions of arboreal pollen during deglaciation along with background trends in biomass burning and radiocarbon dates. Fig. S3 shows the peak frequencies and magnitudes of the high-resolution sites, as well as the number and location of radiocarbon dates in these records.

Data Sources and Locations. Charcoal and pollen data sources, site locations and elevation, and temporal coverage during the Last Glacial–Interglacial Transition (LGIT) are provided in Table S1. Numbers in parentheses after site names are reference numbers. Site locations are shown in Fig. S1 and are coded to reflect the existence of a charcoal peak at 12.9 and 11.7 ka, as determined by the analysis techniques described below.

Chronologies. Lake-sediment records of the kind selected for paleoecological studies have generally well-behaved sedimentation regimes with slowly varying sedimentation rates. This allows chronological control with fewer radiocarbon dates than required for discontinuous terrestrial records, or marine records with continuous or intermittent bioturbation of sediments. For example, the age of a synchronous vegetation change in eastern North America, the *Tsuga* (hemlock) decline, can be estimated with subcentury precision (4750 ^{14}C y BP, with a standard error of the mean of ≈50 y) using networks of lake records like those used here (1, 2). However, owing to the reorganizations of the circulation of the atmosphere and ocean that are involved in the abrupt climate changes, larger than usual uncertainties arise in calibrating radiocarbon ages during the LGIT (3), and so we compared the results from our peak identification analysis based on both a narrow 100-y and wider 500-y window width. As described in the main text, peaks were not more likely to occur at 12.9 than at 11.7 ka in either case.

Analysis of Individual Charcoal and Pollen Records. Charcoal concentration data (particles cm^{-3}) were converted to influx values (particles cm^{-2} y^{-1}) by dividing charcoal values by sample deposition times (y cm^{-1}). For the low-resolution records (>50 y sample^{-1}), we used quantile regression to estimate background charcoal influx values as the 50th percentile (4). The degrees of freedom parameter (df) was 10 for all but 3 records (i.e., 73 for East Lake, 50 for Sharkey Lake, and 6 for Walker Lake).

In continuously sampled (high-resolution), macroscopic (typically >100 μm) charcoal records, large charcoal peaks above background represent individual, local fire events or clusters of events (fire episodes) as has been demonstrated by examination of the portions of the sedimentary records that overlap with dendrochronological or historical records of fire (5, 6). Lower-resolution records based on microscopic charcoal (<100 μm), reflects burning at broader scales (7). Low-resolution records will integrate individual fire episodes, but increased fire activity can still be inferred from large peaks in low-resolution records (8). For Fig. 2 in the main text, any increase in charcoal influx above background within a defined time period (i.e., either ±50 or ±250 y) was considered a "peak."

The high-resolution (<50 y per sample) charcoal influx series were decomposed into background and peaks components using CharAnalysis (9), which allows us to reconstruct peak frequencies and to quantify peak sizes in addition to separating peaks from background charcoal levels (Fig. S3). Charcoal values were interpolated to constant time intervals based on the median resolution at each site. A robust lowess smoother was used to define background trends with a 500-y window width for all but 2 records (sites 18 and 13), which showed an improved signal-to-noise ratio with larger window widths (18). Site 18 was smoothed with a 600-y window and site 13 was smoothed with an 800-y window. Peaks were identified by calculating the residuals above a locally defined threshold. The peaks component was defined as the residuals after subtracting background values from the interpolated series, and charcoal peaks were identified by calculating a locally defined threshold value separating fire-related and non-fire-related variations in the peaks component (9). Only peaks that had a maximum charcoal count with a <5% chance of coming from the same Poisson distribution as minimum charcoal counts within the previous 75 y were considered, except for site 13, 20, and 24, where all peaks were counted due to the lack of the sample volume information required to perform the minimum count test (9, 10). Peak magnitudes were obtained by calculating the positive deviations above the background. Ratios of arboreal to nonarboreal pollen percentages (AP/NAP) were obtained by dividing the sum of arboreal and shrub pollen percentages (AP) by the sum of the total terrestrial pollen percentage [AP/(AP + NAP)]. Changes in AP were used as an indicator of major changes in woody fuel levels, not as a tool for reconstructing detailed changes in vegetation community composition, which is beyond the scope of this article.

Trends in Charcoal Influx, Peak Frequency, and Arboreal Pollen. The estimation of trends in noisy data like the charcoal influx data involves a tradeoff between (*i*) fitting a relatively simple model, like a straight line or polynomial, which allows assessment of the significance of the trend to be made (11) and (*ii*) using a more flexible or "data-adaptive" model which may better represent more complicated or nonlinear forms of a trend, but which makes it harder to establish the overall significance of the trend (12). We use 2 approaches here: (*i*) a piecewise linear or segmented-regression model, which allows some flexibility in the fitted model, in particular changes in slope and intercept at some (possibly unknown) breakpoints, and (*ii*) a local regression or "lowess" approach, which makes no assumptions about the form of the overall trend.

The charcoal influx data were first transformed using the Box–Cox transformation to stabilize the variance of the data as described in Power *et al.* (13). The transformed values were converted to *Z* scores by subtracting the mean value and dividing by the standard deviation using a base period of 15–10 ka to allow comparisons among the records that feature widely varying average charcoal influx rates.

We used the "segmented" package (14) from the R-Project (15) to fit an overall linear trend to the charcoal influx data, allowing for changes in the slope and intercept of the trend line at several breakpoints, which were simultaneously estimated with the trend. There is a tradeoff between the number of breakpoints (and the length of the intervals they define) and the interpretability and robustness of the results. Too few breakpoints may lead to a less-good fit to the data, and greater heterogeneity of the intervals or episodes that are defined, whereas too many breakpoints lead to more complicated ad hoc interpretations of the results and to greater sensitivity of the results to the specific data being analyzed. We explored linear and polynomial (2nd- and 3rd-order) trends, and 2–4 break-

points, with starting values for the breakpoints at even 1,000-y intervals from 11,000 to 14,000 y BP.

The best-fitting model with the fewest parameters was a segmented straight-line model with breakpoints at 12,820 y BP (SE = 128.0 y) and 11,550 yr BP (SE = 162.3 y). Because these breakpoint ages are indistinguishable from the beginning and end of the YDC (12,875 y BP and 11,660 y BP, respectively), we refit this model using the latter values as breakpoints using ordinary least squares "dummy variable" regression. This model is:

$$\begin{aligned} Influx &= 5.241697 - 0.000452 \cdot Age \qquad (Age < 11{,}660 \text{ y BP}) \\ &\quad [0.569100]\ [0.000053] \\ &= -0.797223 + 0.000071 \cdot Age \ (11{,}600\text{–}12{,}875 \text{ y BP}) \\ &\quad [1.034000]\ [0.000084] \\ &= 6.610190 - 0.000512 \cdot Age \qquad (>12{,}875 \text{ y BP}) \\ &\quad [0.625000]\ [0.000045]. \end{aligned}$$

where the values in square brackets are the standard errors of the regression coefficients, and $F = 137$ ($P < 2.2 \times 10^{-16}$), $R^2 = 0.1647$. Note that the slopes of the line segments before (-0.000452) and after (-0.000512) the YDC are virtually identical, but fitting a model that constrains them to be so adds little to the efficiency of the model. Note also that the slope of the line segment during the YDC is not significantly different from zero. This model yields the straight-line segments on Fig. 1*C*, and demonstrates the statistical significance of the overall trend in charcoal influx over the LGIT as well as the absence of a trend during the YDC.

A local-regression or lowess curve (16) was also fit to the data to show the long-term trends unconstrained by the specification of a particular model of the trend. The lowess curve-fitting procedure used the tricube weight function with a fixed-width window of 200 y (100-y half-width) as opposed to a variable-width window that "spans" a fixed proportion of the data points. Fitted values were obtained at "target points" spaced 10 y apart. (Note that this interval is not an expression of our belief in the chronological precision of the data, but simply allows us to graph the fitted values in a reasonable way.) A robustness iteration was used to minimize the influence of unusual points or outliers. We also calculated bootstrap confidence intervals for the lowess curve (1,000 replications) where the sampling-with-replacement was done by sites as opposed to individual samples, to assess the impact of the inclusion or exclusion of specific sites in our dataset. The lowess fitted values appear as the smooth curve in Fig. 1*C*, and the 5th and 95th percentiles of the bootstrapped fitted values define the shaded bands. Note that the segmented-regression trend model and the lowess curve describe the same general trend in charcoal influx during the LGIT.

The density of charcoal peaks in the high-resolution charcoal records (Fig. 1*D*) was displayed by using a kernel density-estimator (17). We selected a bandwidth of 100 y, which provides a compromise between oversmoothing the peak frequencies while still displaying local maxima in peak frequencies that are supported by peaks in multiple individual records. Bootstrap confidence intervals were obtained in the same way as for the influx data.

AP proportions were transformed using the "angular" or arcsine transformation, and a composite curve (Fig. 1*E*) was constructed by smoothing the transformed data in a similar fashion as the charcoal influx data. However, because the temporal resolution of the pollen data are typically less than that of the charcoal data, we used a larger window width (200-y half-width) to smooth these data. Bootstrap confidence intervals were again obtained as for charcoal influx.

The Increase in Charcoal at 13.2 ka. The charcoal increase at 13.2 ka is evident in 14 of the 33 sites recording fires by 13.1 ka (sites 1, 2, 10, 15, 17, 18, 19, 20, 21, 22, 23, 26, 30, and 35; Fig. S2) from 8 different regions. These sites span an elevation range of 8–2,863 m, with 5 sites located above 2,000 m. Similar increases in charcoal influx occurred previously at 3 sites (sites 2, 19, and 21), so the change was unprecedented in only 11 records. Of these 11 records, 13.2 ka marks the beginning of a discrete peak at 7 of them (sites 1, 15, 17, 18, 23, 26, and 30), versus an increase in baseline levels at the remaining 4 sites (sites 10, 20, 22, and 35). Fire frequency also increased to a local maximum at 13.2 ka, after a peak in AP at 13.4 ka (Fig. 2). In contrast, 20 sites show low charcoal influx at 13.2 ka, illustrating that burning was widespread, but not continent-wide at the time.

1. Webb T, III (1982) in *Third North American Paleontological Convention Proceedings* (Montreal), pp 569–572.
2. Bennett KD, Fuller JL (2002) Determining the age of the mid-Holocene *Tsuga cana densis* (hemlock) decline, eastern North America. *Holocene* 12:421–429.
3. Muscheler R, *et al.* (2008) Tree rings and ice cores reveal C-14 calibration uncertainties during the Younger Dryas. *Nat Geosci* 1:263–267.
4. Koenker R (2005) *Quantile Regression* (Cambridge Univ Press, Cambridge, UK).
5. Clark JS (1990) Fire and climate change during the last 750 yr in northwestern Minnesota. *Ecol Monogr* 60:135–159.
6. Whitlock C, Bartlein PJ (2004) in *Developments in Quaternary Science* (Elsevier, Amsterdam).
7. Patterson WA, Edwards KJ, Maguire DJ (1987) Microscopic charcoal as a fossil indicator of fire. *Quat Sci Rev* 6:3–23.
8. Carcaillet C, *et al.* (2001) Change of fire frequency in the eastern Canadian boreal forests during the Holocene: Does vegetation composition or climate trigger the fire regime? *J Ecol* 89:930–946.
9. Higuera PE, *et al.* (2008) Frequent fires in ancient shrub tundra: Implications of paleo-records for Arctic environmental change. *PLoS ONE* 3:e0001744.
10. Gavin DG, Hu FS, Lertzman K, Corbett P (2006) Weak climatic control of stand-scale fire history during the late Holocene. *Ecology* 87:1722–1732.
11. Wigley TML (2006) in *A Report by the Climate Change Science Program and the Subcommittee on Global Change Research*, eds Karl TR, Hassol SJ, Miller CD, Murray WL (U.S. Climate Change Science Program, Washington, DC), pp 129–139.
12. Harvey DI, Mills TC (2003) Modelling trends in Central England temperatures. *J Forecasting* 22:5–47.
13. Power MJ, *et al.* (2007) Changes in fire regimes since the Last Glacial Maximum: an assessment based on a global synthesis and analysis of charcoal data. *Clim Dynam* 30:887–907.
14. Muggeo VMR (2008) Segmented: Segmented Relationships in Regression Models (R Package), Version 0.2-4.
15. R Development Core Team (2008) R: A Language and Environment for Statistical Computing (R Foundation for Statistical Computing, Vienna), Version 2.8.0. Available at http://www.R-project.org.
16. Cleveland WS, Devlin SJ (1988) Locally weighted regression: an approach to regression analysis by local fitting. *J Am Stat Assoc* 83:596–610.
17. Venables WN, Ripley BD (2002) *Modern Applied Statistics with S* (Springer, New York).
18. Higuera PE, Brubaker LB, Anderson PM, Hu FS, Brown TA (2009) Vegetation mediated the impacts of postglacial climate change on fire regimes in the southcentral Brooks Range, Alaska. *Ecological Monographs*, in press.

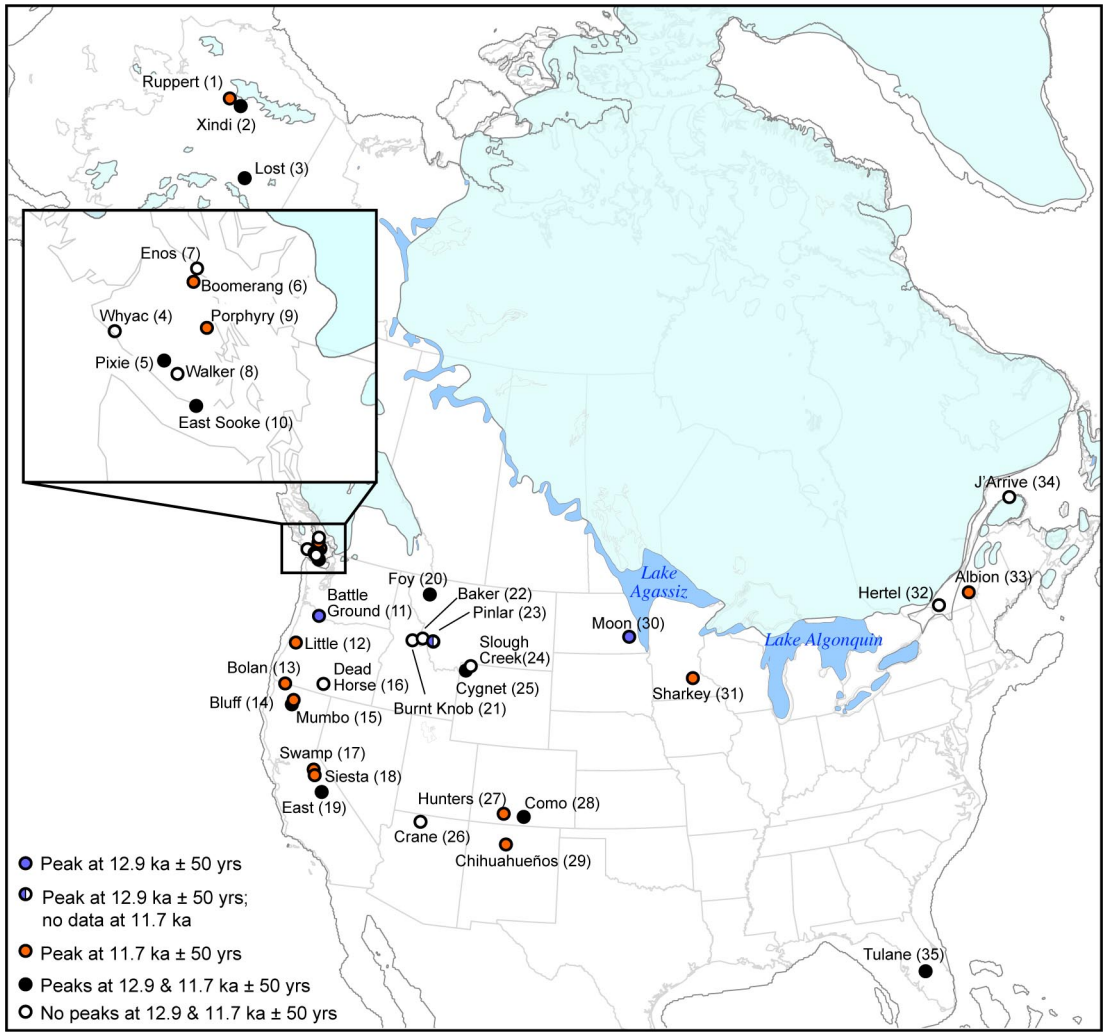

Fig. S1. Paleofire site locations and responses to environmental changes during the Younger Dryas interval (≈12.9–11.7 ka) [Dyke AS, Moore A, Robertson L (2003) *Deglaciation of North America*. Geological Survey of Canada Open File 1547. (Ottawa: Natural Resources Canada.) Available at: www.nrcan.gc.ca.]. Site numbers are in parentheses.

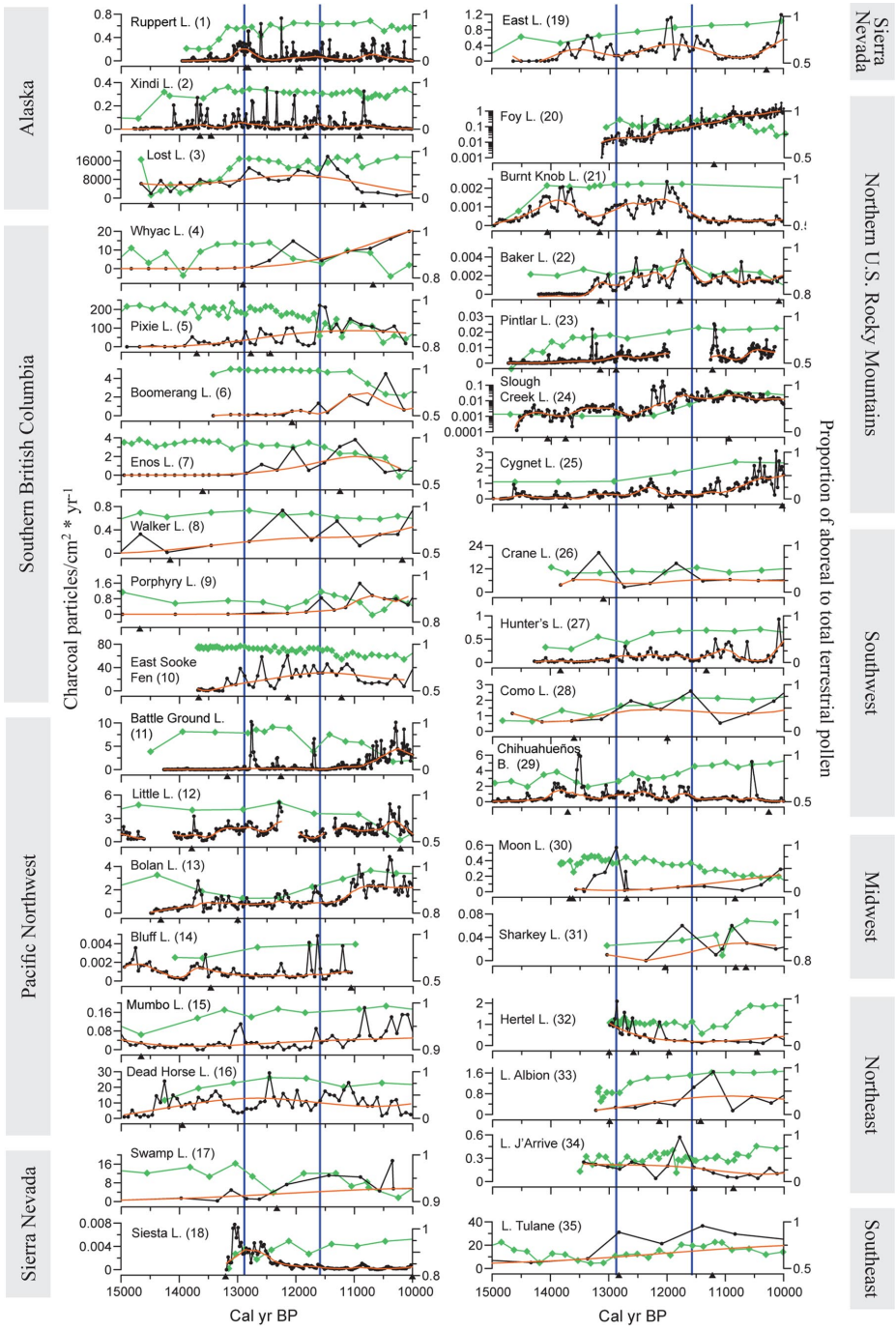

Fig. S2. Reconstructions of biomass burned and woody biomass for 35 sites in North America. Charcoal influx (black line) was smoothed (orange line) to indicate trends in biomass burned. Note the log scales for Foy and Slough Creek lakes. The ratio of arboreal pollen (AP) to total terrestrial pollen (green line) indicates abundance of tree taxa on the landscape, a proxy for woody biomass. AP ranged from ≈0.25 for grassland and herb tundra to 1 for closed forest. Dates based on radiocarbon dating, tephras, or pollen correlations (orange triangles) are also shown. Site numbers follow site names. Records are arranged geographically by region, from northwest to southeast. Vertical blue lines mark the beginning (≈12.9 ka) and end (≈11.7 ka) of the YD.

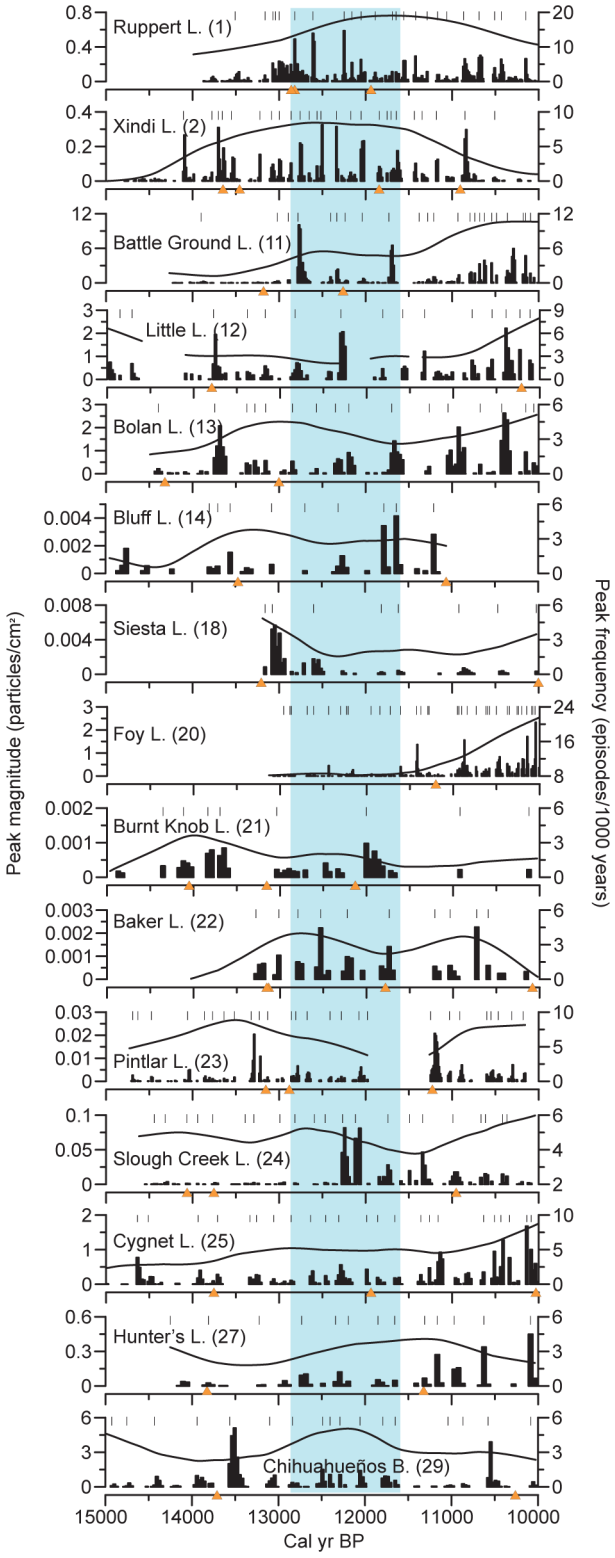

Fig. S3. Fire-regime reconstructions, including peak episodes (tic marks), peak frequencies (smooth black line), and positive deviations above background or peak magnitudes from high-resolution North American charcoal records during deglaciation. Orange triangles are radiocarbon or tephra dates. The Younger Dryas interval is shaded blue.

Table S1. Names, identification numbers, sources, locations, elevations, and time spanned by individual records

ID	Site name	Latitude	Longitude	Elevation, m a.s.l.	Age range (cal yr BP)
1	Ruppert Lake, AK (1)	67.07	−154.23	230	13,078–10,000
2	Xindi Lake, AK (1)	67.11	−152.49	240	15,000–10,000
3	Lost Lake, AK (2)	64.30	−146.69	240	14,650–10,000
4	Whyac Lake, BC (3)	48.67	−124.84	15	15,000–10,000
5	Pixie Lake, BC (3)	48.60	−124.20	70	15,000–10,000
6	Boomerang Lake, BC (4)	49.18	−124.15	360	13,422–10,000
7	Enos Lake, BC (4)	49.28	−124.15	50	15,000–10,000
8	Walker Lake, BC (5)	48.53	−124.00	950	15,000–10,000
9	Porphyry Lake, BC (5)	48.91	−123.83	1100	14,979–10,000
10	East Sooke Fen, BC (3)	48.35	−123.68	155	13,685–10,000
11	Battle Ground Lake, WA (6)	45.80	−122.49	154	14,290–10,000
12	Little Lake, OR*	44.17	−123.58	210	15,000–10,000
13	Bolan Lake, OR (7)	42.02	−123.46	1637	14,545–10,000
14	Bluff Lake, CA (8)	41.35	−122.56	1921	15,000–11,065
15	Mumbo Lake, CA (9)	41.19	−122.51	1860	15,000–10,000
16	Dead Horse Lake, CA (10)	42.56	−120.78	2248	15,000–10,000
17	Swamp Lake, CA (11)	37.95	−119.82	1554	15,000–10,000
18	Siesta Lake, CA (12)	37.85	−119.67	2430	13,241–10,000
19	East Lake, CA (13)	37.18	−119.03	2863	14,634–10,000
20	Foy Lake, MT (14)	48.17	−114.36	1006	13,134–10,000
21	Burnt Knob Lake, ID (15)	45.70	−114.99	2250	15,000–10,000
22	Baker Lake, ID (15)	45.89	−114.26	2300	14,328–10,000
23	Pintlar Lake, MT (15)	45.84	−113.44	1921	14,732–10,000
24	Slough Creek Lake, WY	44.93	−110.35	1884	13,362–10,000
25	Cygnet Lake, WY (16)	44.65	−110.60	2530	15,000–10,000
26	Crane Lake, AZ (17)	36.72	−112.22	2590	13,835–10,000
27	Hunters Lake, CO (18)	37.61	−106.84	3516	14,273–10,000
28	Como Lake, CO (17)	37.55	−105.50	3523	13,602–10,000
29	Chihuahueños Bog, NM (18)	36.05	−106.51	2925	15,000–10,000
30	Moon Lake, ND (19)	46.86	−98.16	456	13,794–10,000
31	Sharkey Lake, MN (20)	44.59	−93.41	305	13,037–10,000
32	Hertel, QC†	45.68	−74.05	70	13,000–10,000
33	Albion, QC (21)	45.67	−71.33	320	13,566–10,000
34	J'Arrive, QC (21)	49.25	−65.38	56	14,055–10,000
35	Lake Tulane, FL (22, 23)	27.59	−81.50	35	15,000–10,000

*C.L., unpublished data.
†P.J.H.R., unpublished data.

1. Higuera PE, *et al.* (2008) Frequent fires in ancient shrub tundra: implications of paleo-records for Arctic environmental change. *PLoS ONE* 3:e0001744.
2. Tinner W, *et al.* (2008) A 700-yr record of boreal ecosystem responses to climatic variation from Alaska. *Ecology* 89:729–743.
3. Brown KJ, Hebda RJ (2002) Origin, development, and dynamics of coastal temperate conifer rainforests of southern Vancouver Island, Canada. *Can J For Res* 32:353–372.
4. Brown KJ, *et al.* (2006) Holocene precipitation in the coastal temperate rainforest complex of southern British Columbia, Canada. *Quat Sci Rev* 25:2762–2779.
5. Brown KJ, Hebda RJ (2003) Coastal rainforest connections disclosed through a Late Quaternary vegetation, climate, and fire history investigation from the Mountain Hemlock Zone on southern Vancouver Island, British Columbia, Canada. *Rev Palaeobot Palynol* 123:247–269.
6. Walsh MK, Whitlock C, Bartlein PJ (2008) A 14,300-year-long record of fire-vegetation-climate linkages at Battle Ground Lake, southwestern Washington. *Quat Res* 70:251–264.
7. Briles CE, Whitlock C, Bartlein PJ (2005) Postglacial vegetation, fire, and climate history of the Siskiyou Mountains, Oregon, USA. *Quat Res* 64:44–56.
8. Mohr JA, Whitlock C, Skinner CN (2000) Postglacial vegetation and fire history, eastern Klamath Mountains, California, USA. *Holocene* 10:587–601.
9. Daniels ML, Anderson RS, Whitlock C (2005) Vegetation and fire history since the Late Pleistocene from the Trinity Mountains, northwestern California, USA. *Holocene* 15:1062–1071.
10. Minckley T, Whitlock C, Bartlein P (2007) Vegetation, fire, and climate history of the northwestern Great Basin during the last 14,000 years. *Quat Sci Rev* 26:2167–2184.
11. Smith SJ, Anderson RS (1992) Late Wisconsin paleoecologic record from Swamp Lake, Yosemite National Park, California. *Quat Res* 38:91–102.
12. Brunelle A, Anderson RS (2003) Sedimentary charcoal as an indicator of late-Holocene drought in the Sierra Nevada, California, and its relevance to the future. *Holocene* 13:21–28.
13. Power MJ (1998) in *Quaternary Studies Program* (Northern Arizona University, Flagstaff, AZ), p 93.
14. Power MJ (2005) Recent and Holocene fire, climate, and vegetation linkages in the Northern Rocky Mountains, USA. PhD dissertation (University of Oregon, Eugene).
15. Brunelle A, Whitlock C, Bartlein P, Kipfmueller K (2005) Holocene fire and vegetation along environmental gradients in the Northern Rocky Mountains. *Quat Sci Rev* 24:2281–2300.
16. Millspaugh SH, Whitlock C, Bartlein PJ (2000) Variations in fire frequency and climate over the past 17000 yr in central Yellowstone National Park. *Geology* 28:211–214.
17. Shafer DS (1989) The timing of Late Quaternary monsoon precipitation maxima in the Southwest United States. PhD dissertation. (University of Arizona, Tuscon).
18. Anderson RR, Allen CD, Toney JL, Jass RB, Bair AN (2008) Holocene vegetation and fire regimes in subalpine and mixed conifer forests, southern Rocky Mountains, USA. *Intl J Wildland Fire* 17:96–114.
19. Clark JS, Royall PD (1996) Local and regional sediment charcoal evidence for fire regimes in presettlement north-eastern North America. *J Ecol* 84:365–382.
20. Umbanhowar CE, Jr, Camill P, Geiss CE, Teed R (2006) Asymmetric vegetation responses to mid-Holocene aridity at the prairie-forest ecotone in south-central Minnesota. *Quat Res* 66:53–66.
21. Carcaillet C, Richard PJH (2000) Holocene changes in seasonal precipitation highlighted by fire incidence in eastern Canada. *Clim Dynam* 16:549–559.
22. Watts WA, Hansen BCS (1988) in *Wet Site Archaeology*, ed Purdy B (Telford, Caldwell, NJ).
23. Grimm EC, *et al.* (2006) Evidence for warm wet Heinrich events in Florida. *Quat Sci Rev* 25:2197–2211.